

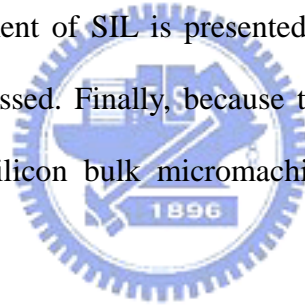
Chapter 2

Principle

2.1 Introduction

The basic theories of the proposed fiber-based integrated optical pickup module are discussed in this chapter. The module consists of three parts: fiberlens, v-groove and solid immersion lens (SIL). The characteristics of each component are discussed. The detailed simulation results of all components are presented in next chapter.

First, the paraxial Gaussian beam (ABCD) is used to calculate the spot size in fiberlens. Then the development of SIL is presented and the basic principle of SIL based optical system is discussed. Finally, because the V-groove and the 45 degree mirror can be realized by silicon bulk micromaching, the theory of silicon bulk micromaching is presented.



2.2 Fiberlens

The fiberlens is designed with a large radius R . The distance between the SMF and the microlens is filled with a pure silica rod of the same diameter and same refractive index as the core of the SMF to avoid reflection, as shown in Fig. 2-1. The mode field radius W_0 is computed by the following formula [1].

$$\frac{W_0}{a} = 0.65 + \frac{1.619}{V^{3/2}} + \frac{2.879}{V^6} \quad (2-1)$$

Where a is the core radius of the step-index fiber, and V is the normalized frequency

$V = \frac{2\pi}{\lambda} a \sqrt{n_1^2 - n_2^2}$ (n_1 and n_2 , are the refractive indices of the core and cladding, respectively). The mode field diameter $2W_0$ at wavelength $\lambda = 0.63 \mu\text{m}$ is about $4.3 \mu\text{m}$.

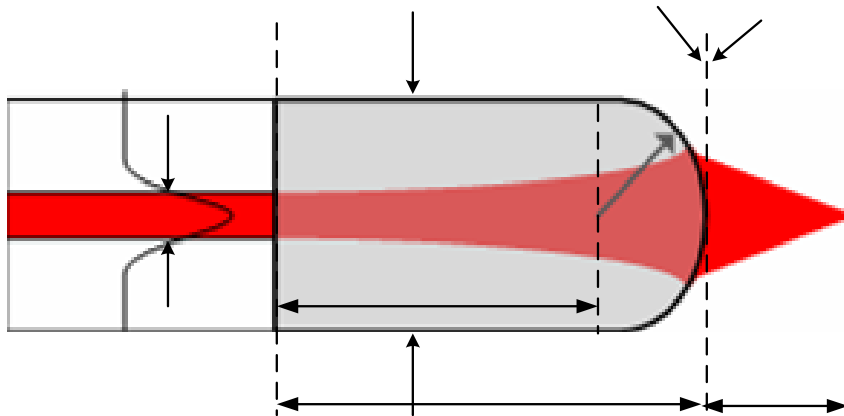


Fig. 2-1 Illustrated schematics of the microlens on the end face of the SMF (refractive index of the silica rod $n = 1.47$, cladding diameter $2a = 125 \mu\text{m}$, mode field diameter $2W_0 = 4.3 \mu\text{m}$ at $\lambda = 0.63 \mu\text{m}$).

For the thick microlens system by ABCD law, W_1 and r_1 , beam waist and radius at output plane RP_{OUT} (Plane 1) can be expressed as

Mode field diameter
 $2W_0 = 4.3 \mu\text{m}$

$$W_1 = W_0 \sqrt{1 + \left(\frac{g}{Z_R}\right)^2} \quad (2-2)$$

and

$$r_1 = g + \frac{Z_R^2}{g} \quad (2-3)$$

Where W_0 is the mode field radius of an SMF, g is the propagation distance from RP_{IN} (Plane 0) to RP_{OUT} , and Z_R is the Rayleigh range where

$$Z_R = \frac{\pi W_0^2 n}{\lambda} \quad (2-4)$$

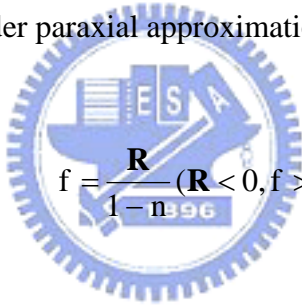
After passing through the end face of the silica rod, the radius of the beam size W_2 and the curvature r_2 at Plane 2 becomes

$$W_2 = W_1 \quad (2-5)$$

and

$$r_2 = \frac{r_1 f}{f - r_1} \quad (2-6)$$

Where f is the focal length under paraxial approximation given by



$$f = \frac{R}{1 - n} \quad (R < 0, f > 0) \quad (2-7)$$

Where R is the radius of the plano convex lens on the fiber front end. Thus, the focused beam waist W_i and working distance Z_i can be written as

$$W_i = \frac{W_2}{\sqrt{1 + \left[\frac{\pi W_2^2}{\lambda r_2} \right]^2}} \quad (2-8)$$

and

$$Z_i = \frac{-r_2}{\sqrt{1 + \left[\frac{\lambda r_2}{\pi W_2^2} \right]^2}} \quad (2-9)$$

respectively.

A hemispherical microlens at the front end is used as a focusing element. The length of the pure silica rod d is designed to control the focused beam waist W_i , which is defined as half-width at $1/e^2$ maximum intensity, and position Z_i , which is defined as the distance from the beam waist position to the lens front end. The relationship of W_i and Z_i is a function of propagation distance $g = d + \mathbf{R}$, where \mathbf{R} is the radius of the hemispherical lens. The detail result is shown in next chapter.

2.2 Solid immersion lens (SIL) system

Solid Immersion Lens (SIL) systems are attractive because they produce spots smaller than conventional optical systems with high throughput to the recording layer. The areal density achievable with conventional optical recording technology is determined by the diffraction limit. The minimum focused spot diameter (full-width at $1/e^2$) is approximately λ/NA_{EFF} , where λ is the free space wavelength and $NA_{\text{EFF}} = n\sin\theta$ (n is the refractive index of the image space, and θ is the marginal ray angle). Typically, the NA_{EFF} is ~ 0.5 in air and the minimum diameter of the optical spot is in the order of λ .

The diffraction limit can be circumvented by the use of near-field optics. In 1984 Pohl *et al* [2] demonstrated a near-field optical microscope using a glass rod tapered down to a small pinhole and covered it with a deposited metal film. To obtain a resolution comparable to the diameter of the pinhole, the pinhole must be placed from the sample within a distance comparable to the pinhole size. Betzig *et al.* [3] used a tapered fiber with a pinhole at the end to demonstrate a resolution of 60 nm with a 488 nm light source. Hosaka and others [4] utilized near-field optics to record in phase-change (PC) media and achieved a minimum recorded mark of 60 nm with a

785 nm laser. One major issue of using these tapered fibers is the high transmission loss of the light; (throughput is approximately $10^{-3}\sim 10^{-4}$ with the aperture diameter of 100 nm [5]).

An alternative approach with solid immersion lens (SIL) proposed by Kino *et al* [6-7] provided a scanning image directly, required no mechanical scanning, had a higher light budget, and could be easily added onto an existing optical data storage system. Therefore, SIL-based optical systems are more feasible than other near-field techniques in the high-data-rate optical storage applications [8-9].

A hemispherical solid immersion lens (SIL) system shown in Fig. 2-2 includes an objective lens and an SIL which is nearly in contact with the sample. The incident light is focused with a marginal angle θ at the hemispherical center of a high-refractive-index SIL without refraction. The NA_{EFF} of the system is increased by a factor n , where n is the refractive index of the SIL. Therefore, the focused spot size becomes smaller and the mark density becomes higher:

$$\text{spot size using hemispherical SIL} = \text{spot size} / n \quad (2-10a)$$

$$\text{effective NA} = n \times \sin \theta \quad (2-10b)$$

In the case of $NA_{EFF} > 1.0$, this setup becomes a near-field approach. The outer rays exceeding the critical angle ($\theta_c = \sin^{-1}1/n$) are totally internally reflected at the air/SIL interface and the field associated with them falls off exponentially away from the interface. This will degrade both the focused spot and the reflected signal.

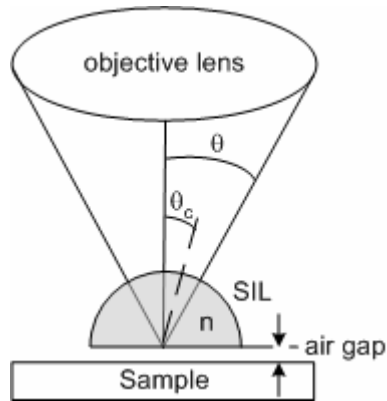


Fig. 2-2 Hemispherical SIL focusing at the bottom surface.

The SIL-based system is often used when the sample is placed within 100 nm from the SIL with visible light. For example, the 1/e decay distance $d_{1/e}$ of the evanescent energy at NA_{EFF} is given by [8]:

$$d_{1/e} = \frac{\lambda}{4\pi} \frac{1}{\sqrt{NA_{EFF}^2 - 1}} \quad (2-10)$$

For $\lambda = 650$ nm and $NA_{EFF} = 1.2$, $d_{1/e} \cong 115$ nm.

Further improvement can be achieved by using a stigmatic focusing lens, as illustrated in Fig. 2-3 (a). In this case, the converging cone of light aimed at a distance $n \times a$ below the center of a sphere (with radius a and refractive index n) will focus a diffraction-limited spot at the distance a/n below the sphere center after the refraction, and the NA_{EFF} can be increased by a factor of n^2 , not only because the wavelength within the super SIL is shortened by a factor n , but also the sine of the cone angle,

$\sin\theta$, is increased by a factor of n . Therefore, the spot size is reduced by the same factor:

$$\text{spot size using super SIL} = \text{spot size} / n^2 \quad (2-11a)$$

$$\text{effective NA} = n^2 \times \sin \theta \quad (2-11b)$$

However, the full factor of n^2 mentioned above cannot be realized without any limitation since the bending of the marginal ray within SIL cannot exceed 90° , as shown in Fig. 2-3 (b). The super SIL can only increase its $\sin\theta$ up to 1, at which the remaining rays will miss the super SIL. Thus this limits the NA of the objective lens to $1/n$ and the maximum NA_{EFF} of the super SIL system is $n\text{NA}$, and not $n^2\text{NA}$.

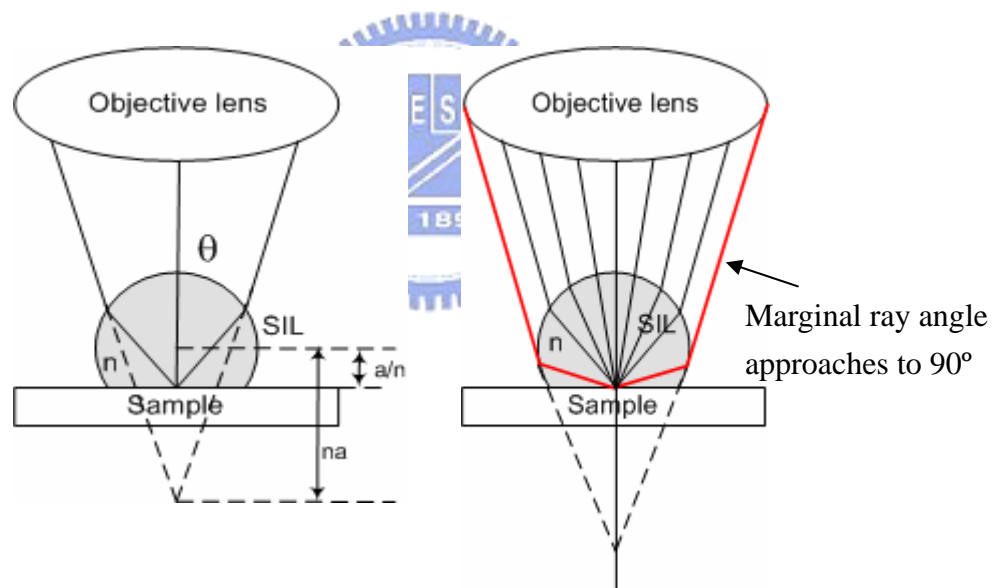
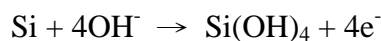


Fig. 2-3 (a) Super SIL and (b) the marginal ray angle approaches 90° with respect to the image space.

2.3 Si bulk micromachining

Wet anisotropic chemical etching of silicon is one of the key technologies in silicon micromachining. The simplest and most widely used micromachined structure for fiber applications is an anisotropically etched V-groove on a (100) silicon wafer. The groove is defined by {111} planes that are slanted at 54.7° to the surface. The side walls of the groove can act as mirrors. There are applications where a 45° mirror plane at the end of the groove is needed to provide a right angle change for the light path. Because of the precise orientation between different crystal planes, anisotropic etching can be used to fabricate precise three dimensional structures such as 45° mirror on the (110)-planes. Wet chemical etching in pure KOH (potassium hydroxide), EDP (ethylene diamine-pyrocatechol), TMAH (tetramethyl ammonium hydroxide), N_2H_4 (hydrazine), or KOH with isopropyl alcohol (KOH/IPA) is known to etch different crystal planes at different etching rates. The main reaction equations for all the mentioned etchants are described as following:

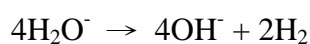
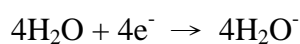
1. Silicon atoms act with OH^- on the surface



2. $Si(OH)_4$ in step 1. dissolves in the solution when $pH > 12$



3. Four e^- in step 1. act with H_2O



described above, OH^- and H_2O are the main substances in the reactions. The other additives, such as pyrazine or 2-propanol (IPA), will cause the change in etching rate.

Most of the reported anisotropic etchants are aqueous alkaline solutions, either organic or inorganic. Among them the most widely used is KOH. The anisotropy is strongly dependent on the etchant composition, etchant concentration, dopant concentration, temperature and even stirring. Because the smoothness of the etched surface can be improved by adding IPA to pure KOH solution, the KOH/IPA etchant is used to fabricate the (110)-groove with sidewalls at 45° angles to the surface of the (100)-oriented silicon substrate.

Crystalline silicon forms a covalently bonded structure, the diamond-cubic structure, which has the same atomic arrangement as carbon in diamond form and belongs to the more general zinc-blend classification. Silicon, with its four covalent bonds, coordinates itself tetrahedrally, and these tetrahedrons make up the diamond-cubic structure. This structure can also be represented as two interpenetrating face-centered cubic lattices, one displaced $(1/4, 1/4, 1/4)a$ with respect to the other, as shown in [Fig. 2-4](#).

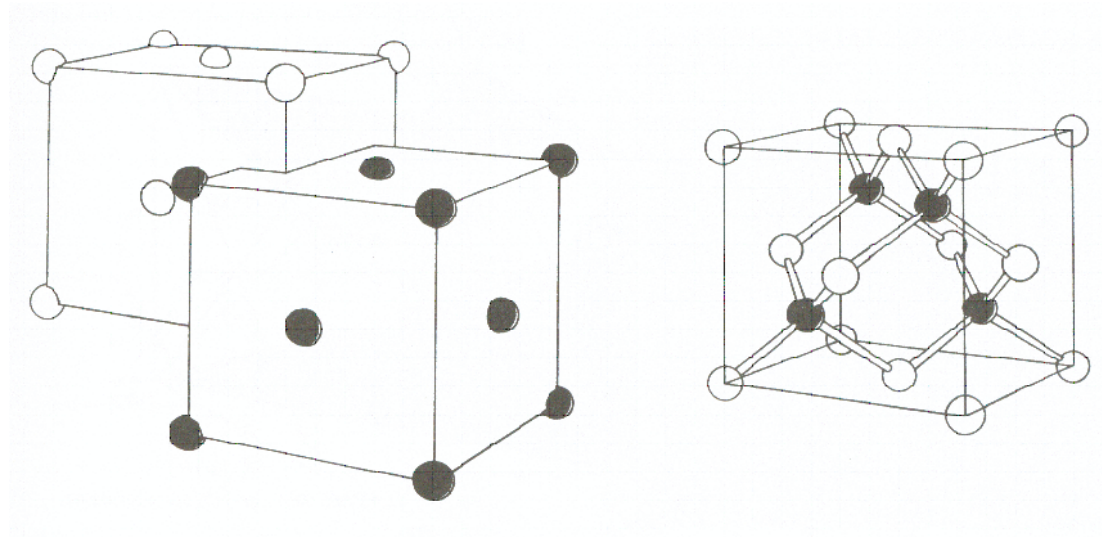


Fig. 2-4 The diamond-type lattice can be constructed from two interpenetrating face-centered cubic unit cells. Si forms four covalent bonds, making tetrahedrons.

For such a cubic lattice, direction $[hkl]$ is perpendicular to a plane with the Miller indices (hkl) . The lattice parameter 'a' for silicon is 5.4309\AA . Its diamond-cubic lattice is surprisingly wide open, with a packing density of 34%, compare to 74% for a regular face-centered cubic lattice. The $\{111\}$ planes present the highest packing density and the atoms are oriented such that three bonds are below the plane. $\{111\}$ planes always have lowest etching rate for all the etchants because of its highest packing density.

In **Fig. 2-5**, the unity cell of a silicon lattice is shown together with the correct orientation of a $[100]$ -type wafer relative to this cell. It can be seen from this figure that intersections of the nonetching $\{111\}$ planes with the $\{100\}$ planes are mutually perpendicular and lying along the $\langle 110 \rangle$ orientations. Provided a mask opening (a rectangular or a square) is accurately aligned with the primary orientation flat, i.e., the $[110]$ direction, only $\{111\}$ planes will be introduced as sidewalls from the very beginning of etching, as shown in **Fig. 2-6 (a)**.

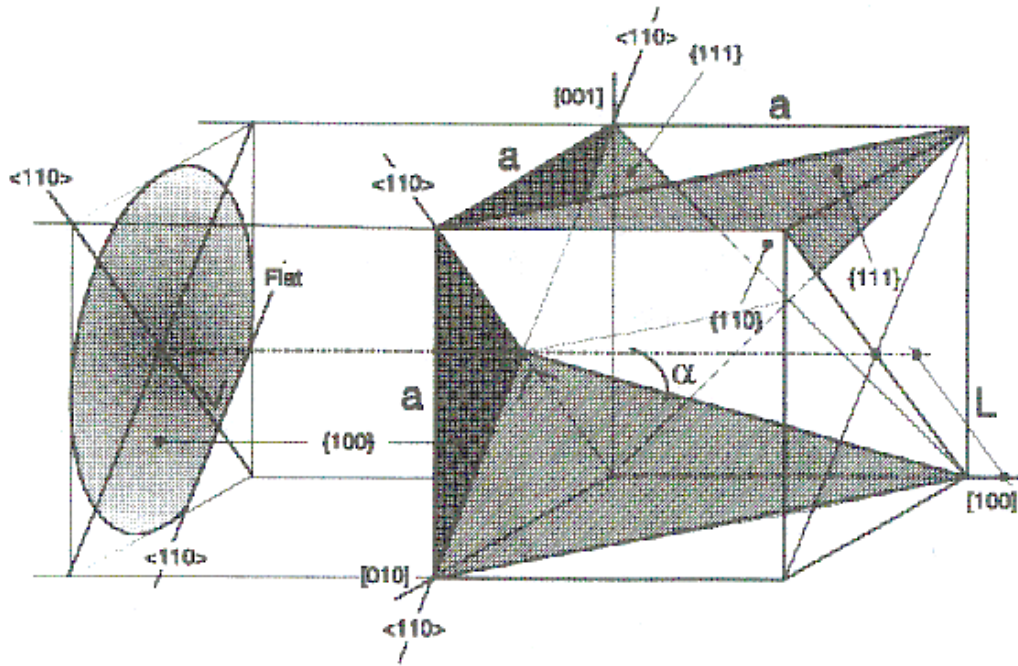


Fig. 2-5 (100) silicon wafer with reference to the unity cube and its relevant planes

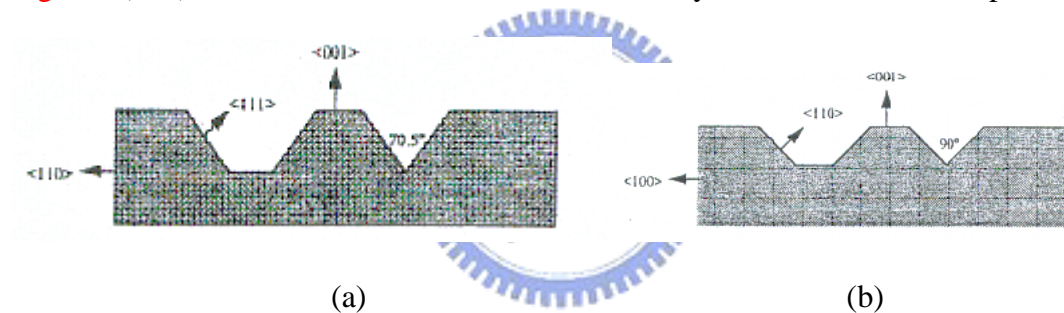


Fig. 2-6 (a) V-groove formed by the mask opened parallel to (110)-flat
 (b) 90° V-groove formed by the mask opened parallel to (100)-flat

By aligning the mask accurately with the (010)-flat, i.e., 45° to (110) primary orientation flat, and choosing the anisotropic etchant with a selectivity of (100)/(110) > 1, a 90° V-groove bounded by (110) sidewalls can be obtained, as shown in Fig. 2-6 (b). Furthermore, the (110)-plane can be used as a 45° mirror for its orientation on (100) wafer and its smoothness.

2.5 Summary

In this chapter, the paraxial Gaussian Beam (ABCD) was described in fiberlens. In hemispherical SIL, the spot size by hemispherical SIL is decreased by the refractive index, n , and effective NA is increased by the refractive index, n . In super SIL, spot size by super SIL is decreased by the refractive index square and effective NA is increased by the refractive index square. The theory of silicon bulk micromachining was presented. The overall simulation will be discussed in next chapter.

